Journal of Structural Geology, Vol. 12, No. 1, pp. 113 to 121, 1990
Printed in Great Britain

0191–8141/90 $03.00+0.00

Allochthony of the Chartreuse Subalpine massif: explosion-seismology constraints

F. THOUVENOT and G. MÉNARD

L.G.I.T., Observatoire de Grenoble, I.R.I.G.M., B.P. 53X, 38041 Grenoble, France

(*Received* 28 *July* 1988; *accepted in revised form* 6 *June* 1989)

Abstract—The deep structure of the Chartreuse Subalpine massif has been investigated with explosion-seismology techniques involving several longitudinal and fan profiles. The main results obtained suggest evidence of a refraction level at shallow depth (2 km) and three deep-seated reflectors (4.5, 8 and 10 km). The shallow level could be the Urgonian limestone slab; the three deep reflectors could be associated with autochthonous and parautochthonous pre-Triassic basements. The discussion of these results mainly concerns the tectonic significance of the shallow, unambiguous refractor: detailed balanced cross-sections of the massif request the presence of a new major overthrust in the sedimentary filling of the Subalpine chains. With an extent of at least 15 km, it opens up wide possibilities for oil traps in the Tertiary molasse underneath.

INTRODUCTION

MOST geologists are well aware of the extensive use of vertical-reflection seismics to detail the structure of sediments and to map the crystalline basement. The success of the method is to shade off the contribution of explosion seismology, where shots are observed by autonomous stations at distances of a few tens of km. Such seismological data on the deep structure of sediments are uncommon, more so in zones of complex tectonics. Those zones expose surface outcrops where the tectonic evolution is often not clear-cut, which may lead to different interpretations. Being key zones for structural geologists, they were obvious sites for making balanced cross-sections, even if the information which could be integrated was mainly superficial.

The Alpine foreland (Fig. 1), richly described by surface observations, can be considered such a key zone, but with very poor structural constraints at depth. This paper shows kinds of data which can be derived by explosion seismology in such a complex zone, where other information is absent. In the vicinity of the external crystalline massifs (ECMs), the position of the pre-Triassic basement is far from clear, data being scarce and their interpretation ambiguous. Available isobath maps, for instance the ones compiled by Ryback *et al.* (1978) for the Swiss part and by Ménard (1980) for the French part, postulate the overthrust of the Belledonne, Aiguilles Rouges and Aar ECMs towards the NW. The thrust plane, dipping towards the inner Alpine arc, implies the existence of a great peri-Alpine trough, a subsiding zone produced by the bending of the European plate (Karner & Watts 1983, Mugnier & Ménard 1986, Mugnier & Vialon 1986).

This hypothetical overthrust was taken into account when interpreting the ALP75 explosion-seismology experiment, where about 200 stations were deployed along an 850-km-long profile following the axis of the Alps (Alpine Explosion Seismology Group 1976). The western segment of this lithospheric profile extended from the Bauges Subalpine massif to the Aiguilles Rouges ECM. Its record section displayed very clear high-energy late arrivals; this phase was even the most prominent one in the 30–40 km range (Thouvenot & Perrier 1981). These energetic onsets were interpreted as reflections from the basement, indicating a very thick sedimentary trough bottoming at 10 km under the Lake of Annecy depression. Structural cross-sections of the Helvetic and Dauphinois zones now take this postulated trough into account, even if there is a clear lack of data about its exact shape.

The ECORS-CROP vertical-reflection seismic line across the Jura and the Alps should soon provide new data concerning the deep structure of the northern Subalpine chains in the Bornes area. To complement this action, farther south, we chose the Chartreuse massif as a test site for our explosion-seismology experiment. Specifically aimed at revealing the deep structure, this experiment is part of a broad research programme including the study of the deep structure of the Vercors massif (Arpin *et al.* 1988) and the Provence chains (Biberon 1988): any additional seismic information for the Subalpine chains is believed to be another geometric constraint when testing new, comprehensive, orogenic models.

THE EXPERIMENT

The use of Chartreuse as a test site was dictated by its situation near the central part of Belledonne. If we assume that the Alpine foreland tectonics developed as a result of the ECM crustal overthrust towards the NW (Ménard 1979), we can expect the basement as well as intrasedimentary discontinuities to dip towards the SE or NW, with a uniform NE strike. Moreover Chartreuse

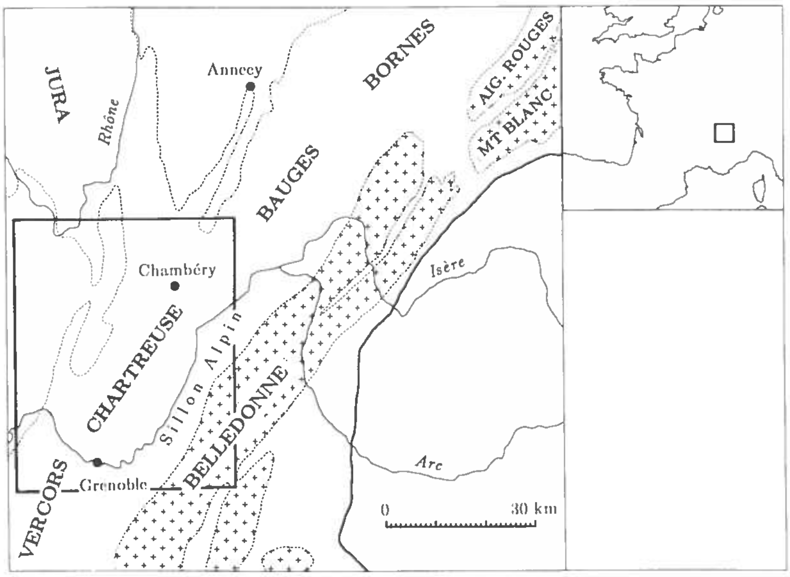

Fig. 1. General simplified map of the north-western Alpine domain. Heavy line marks the Penninic Frontal Thrust. Inset shows position in France. Box shows position of detailed map (Fig. 2). Crosses mark crystalline massifs.

is easy to reach, at least along its eastern flank—*Balcon de Chartreuse*—and along its central syncline. Finally, we derived benefit from the relative narrowness of the *Sillon Alpin* between northern Chartreuse and Belledonne: the Isère valley, with its thick Quaternary sedimentation, is seismically very noisy and it proved sensible to reduce, as far as possible, the number of seismic stations on the alluvia.

The field layout (Fig. 2) consisted of two longitudinal and two fan profiles with a unique shot-point located at

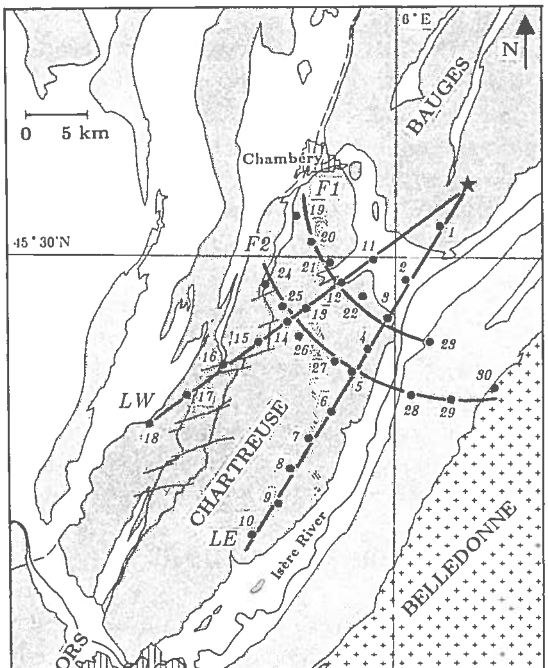

Fig. 2. Situation map of the explosion-seismology experiment, with the shot-point in the Bauges massif (star) and the recording stations (full circles) arranged along two in-line profiles (LE and LW) and two fan profiles (F_1 and F_2). Shaded: Mesozoic terrains.

La Thuile in the south of the Bauges massif, on the other side of the Chambéry cross-valley. Boreholes for the 300 kg shot were drilled into marly-calcareous formations. The two 30-km-long profiles LE and LW run through a variety of series from the Bathonian to the Senonian. Fan profile F_2 reaches the *Rameau Externe* of Belledonne on the eastern bank of Isère. The Liassic and Jurassic cover of Belledonne was sampled meanwhile between the river and the crystalline outcrop. Except for one station installed on micaschists, the same kind of marly-calcareous sediment was found at every recording-point.

We used 30 stations of the deep-seismic-sounding type: 2 Hz three-component geophones, window-triggered FM magnetic recording, off-line digitization and processing. The failure rate—disability of the automatic equipments to record the shot correctly—reached as high as 20%. This resulted in gaps in the profiles where, unfortunately, the lack of data is severely felt. The mean altitude of the stations (855 m) is used as the datum plane to which the computed depths are referred.

SEISMIC RESULTS

In-line profiling

The two longitudinal record-sections are presented in Figs. 3 and 4 with the shot-point being set on the right-hand side of the section. In-line profiles are thus looked at from the SE. A reduction velocity of 6 km s^{-1} is used for the display.

Because the shot-point and the nearest station were situated on a plateau overlooking the Chambéry cross-valley, topographic effects prevented the direct wave d, which propagates through Neocomian marly-calcareous formations, from being observed farther on. Its mean velocity of 4.5 km s^{-1} was consequently ill-constrained.

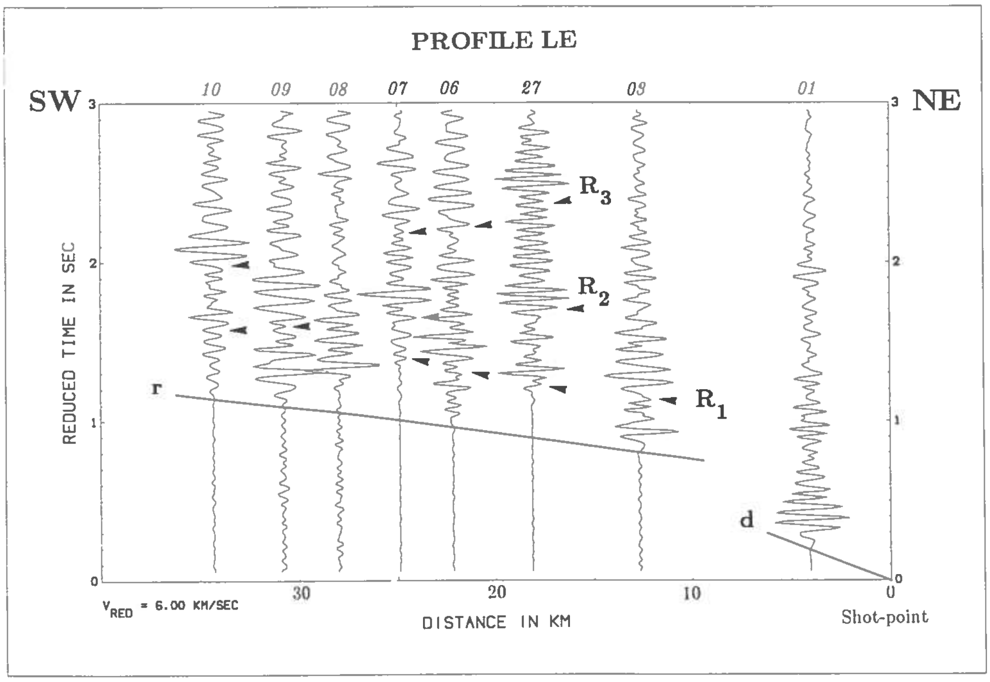

Fig. 3. Record-section along in-line profile LE with a reduction velocity of 6 km s^{-1}. The wave pattern consists of five groups: the direct wave d; a wave r refracted from a shallow level (2 km); and three waves reflected from different levels within the sediments or the upper crust (4.5, 8.5 and 11 km).

A refracted wave r can be followed in first arrival on both profiles from ≈12 km onwards; this head wave has a velocity of ≈5.3 km s^{-1}. Such high velocities were previously measured for the Mesozoic sediments in the Bauges and Aravis Subalpine massifs, where Thouvenot & Perrier (1981) found a mean value of 5.4 km s^{-1}. Vercors Urgonian limestone slabs, when sounded with a seismic-hammer method, also yielded very high velocities, up to 5.7 km s^{-1} (Thouvenot 1981). This refractor is interpreted as a compact and homogeneous limestone horizon at a mean depth of 2 km referred to the datum plane.

In Figs. 3 and 4, the first arrivals corresponding to the r refractor are often very faint, as frequently happens with a head wave. For instance, station 07 in Fig. 3 shows such a poor onset, even if a careful close-up removes the ambiguity. In such profiles, the correlation of late arrivals is even more confusing. The reason is three-fold: (i) only eight stations could be deployed along each line, which is obviously inadequate; (ii) we were interested here in relatively shallow discontinuities, whereas the mean frequency of the signals (≈20 Hz) provided a resolution of 250 m (this meant that we were unable to separate the seismic effects of two close-set disconti-

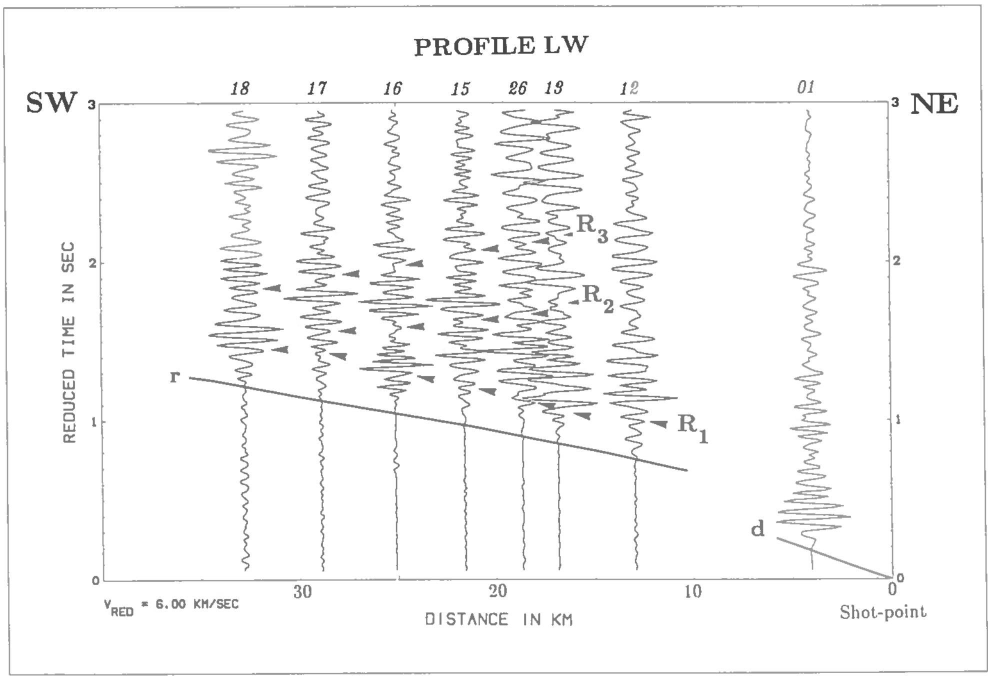

Fig. 4. Record-section along in-line profile LW with a wave pattern similar to profile LE.

nuities); (iii) finally, we were aware that the heterogeneity of the Alpine foreland did not bode well for observing clear correlations of late arrivals.

Even if energetic wave trains are obvious on the record-sections, there are of course many different ways to correlate them, especially when a phase can only be followed sporadically, due to the poor coverage of the observation array. However, our correlations are constrained by the fact that reflected wave travel-time curves *cannot* have any position in the record-section (Sheriff & Geldart 1982). (This is quite different from what happens with vertical-reflection seismics where a stacked section shows many differents reflectors with different dips at different places.) Moreover, as the seismic stations were equipped with three-component geophones, vertical-displacement record-sections were complemented here with horizontal-displacement record-sections. Fan profiles (see next section) were helpful too, because one had to correlate on the longitudinal record-sections phases which had to be apparent on the fan record-sections, and vice versa. Altogether, this correlation step can be considered a jig-saw puzzle where different pieces could only be assembled in a given way and where a propagation of the constraints—in the sense of artificial intelligence (Winston 1981)—had to be taken into account.

Using the assumption that a reflection will produce either an energetic wave train or at least an alteration of the preceding wave train, three reflected waves have been correlated on both profiles. Reflection R_1 comes first. Observed in the 10–30 km range, it provides very consistent values for depth (4.5 km) and surface-to-reflector velocity ($\approx$4.8 km s^{-1}). Reflection R_2 is observed at distances greater than 15 km. The surface-to-reflector mean velocity is slightly different—5.2 km s^{-1} for LE, 5.1 km s^{-1} for LW—which provides two different depths: 8.5 and 7.5 km, respectively. Although these results show a dip of the reflector to the SE, as could be expected from the tectonics, the poor constraint we have on velocities does not allow a decisive answer. Finally, reflection R_3 slightly increases the mean velocity value: 5.25 km s^{-1} for LE and 5.2 km s^{-1} for LW. Again, this makes the reflector slightly deeper under the eastern profile (11 km) than under the western profile (10 km).

Fan-shooting

Two fan profiles recorded the shot at constant distances of 12 km for F_1 and 18 km for F_2. These values were chosen to benefit from the theoretical maximum of amplitude reached by critical reflections (Sheriff & Geldart 1982), from interfaces in the 4–8 km depth range. In the Alps, this kind of fan-shooting has already proved successful for deep reflectors (ECORS-CROP Deep Seismic Sounding Group 1989a,b). In the present case, both fans are beyond the cross-over distance for the 2 km deep refractor, so that the first arrival corresponds to a wave refracted from this level.

A common feature of the fan-shooting results (Figs. 5–7) is the azimuthal scale: as seen from the shot-point, each station is in a given azimuth and the seismic trace is consequently plotted on the record-section. Actually, this azimuthal scale is reversed, because we found it more convenient to have a view from the SW. This means that the record-sections are along NW–SE transverse lines and, as we also reversed the time scale, they

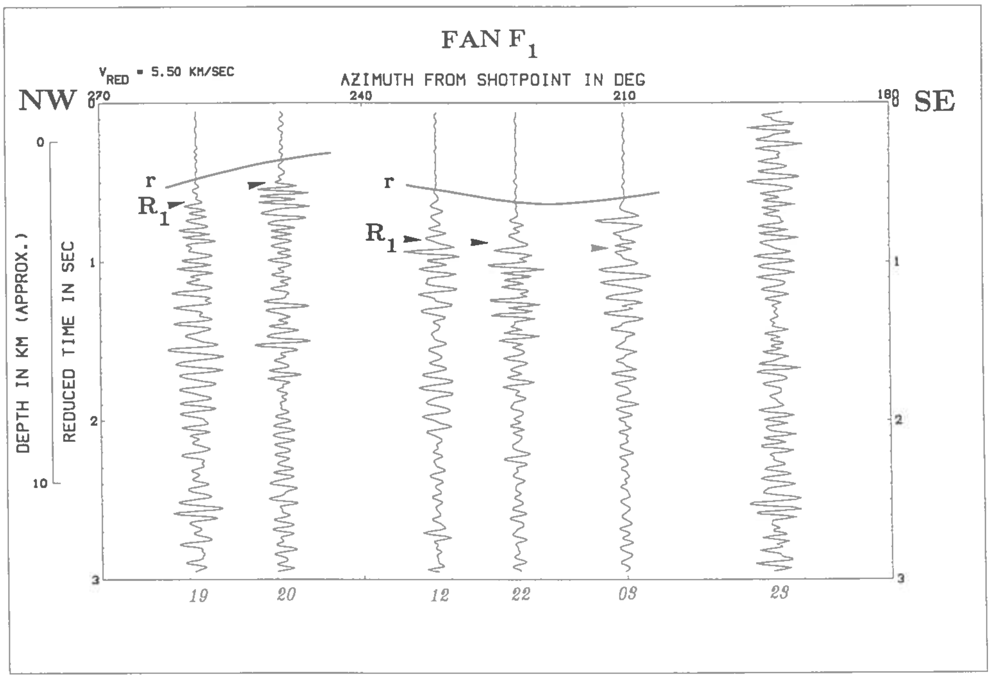

Fig. 5. Record-section along fan F_1 mean offset 12 km, with a reduction velocity of 5.5 km s^{-1}. Azimuths are plotted horizontally and the time scale is reversed, which provides a NW–SE cross-section. The refracted wave and reflection R_1 both exhibit strong variations corresponding to level differences reaching 2 km. Reflection R_2 can be estimated at about 1.5 s in reduced time; the R_3 reflector is too deep to allow any observation along this close-offset fan.

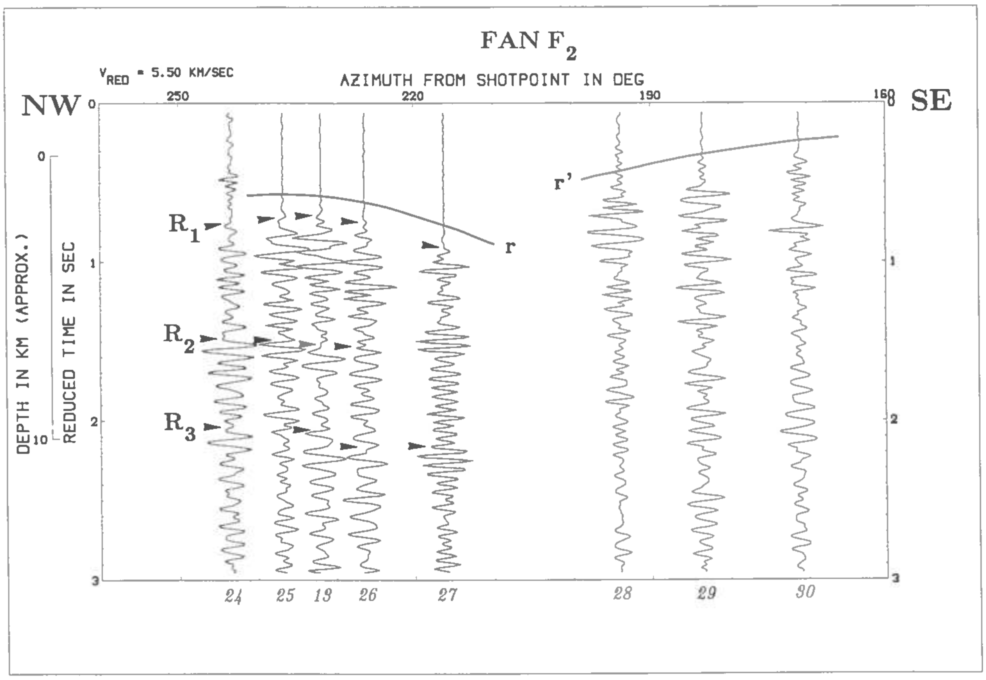

Fig. 6. Record-section along fan F_2 mean offset 18 km, with a reduction velocity of 5.5 km s^{-1}. Observations are similar to fan F_1, with now a faint reflection R_3. The time shift of seismic traces in the eastern part of the section is a consequence of the shallow position of the crystalline basement ahead of Belledonne (≈1.5 km).

can be looked at as cross-sections of northern Chartreuse. Figures 5 and 6 show these cross-sections for fans F_1 and F_2, respectively. Here a reduction velocity of 5.5 km s^{-1} is used to prevent unavoidable deviations from the theoretically constant shot-point-to-station distance (subsequently called *offset*) spoiling the reflector alignments. This value of 5.5 km s^{-1} is actually the mean apparent velocity value for the reflections we are interested in. Figure 7 shows the same data for fan F_2 plotted in the depth domain instead of the time domain, which provides a more readily usable cross-section. The mean

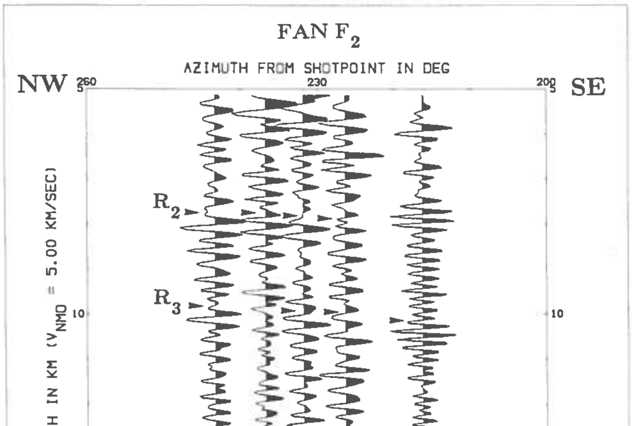

Fig. 7. Record-section along fan F_2 converted to the depth domain, with a normal move-out velocity of 5.0 km s^{-1}.

velocity above the reflectors (normal move-out velocity) is 5.0 km s^{-1}. However this, of course, would make the depth scale slightly inaccurate at very shallow depth—which explains why Fig. 7 is restricted to the 5–15 km depth range only.

Fan F_1 (Fig. 5) shows time variations in the first onset (refracted wave). Station 20 is, for instance, 0.3 s earlier than station 22. Shifting to the depth domain, this implies the refractor to be very shallow in the western part and deeper in the eastern part (depth computations are given later). Because the structures were sampled too loosely, it is difficult to decide whether this refraction level is continuous with a top around station 20 or if there is a fault between station 20 and station 12. The geometric and tectonic implications of such a feature are particularly important. A similar time-offset is also observed for reflection R_1. The reflection level rises gently to the west in the central part of the section, at depths ranging from 5.4 to 5.0 km; then, it is shifted upwards on the westernmost traces to reach a top depth of 3 km. It can be seen from the in-line displays (Figs. 3 and 4) that reflection R_2, because of its depth of 7 km, cannot be traced reliably for small offsets (the smaller the incidence angle on the reflector, the more difficult the reflection will be to detect). Fan F_1, with its offset of 12 km, is hence *a priori* not adapted to observe this reflection, let alone reflection R_3 which is even deeper. However, the westernmost traces of fan F_1 (Fig. 5) show that, even if we are unable to clearly discern reflector R_2, an obvious energy arrival can be observed in the corresponding depth range (≈7 km).

Fan F_2 (Fig. 6) shows another clear variation in arrival times for the refraction onset and for reflection R_1. The top position is shifted to the east, between stations 25

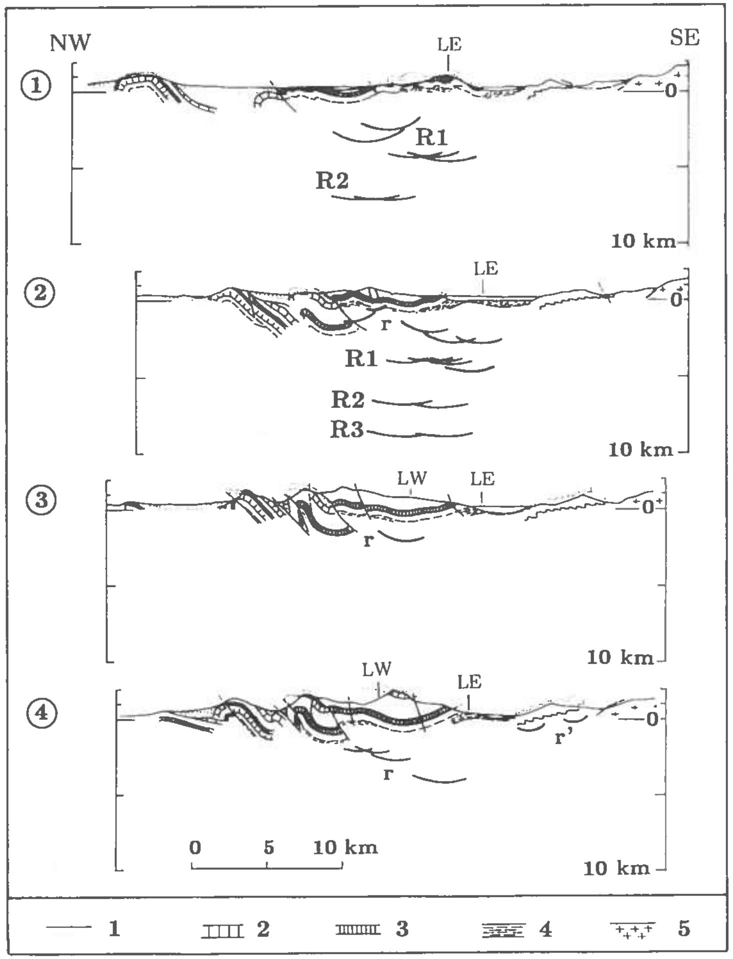

Fig. 8. Four NW–SE cross-sections of northern Chartreuse (see map, Fig. 10), with the surface geology and the position of the refraction and reflection levels: r,r′ = refractions; R_1, R_2 and R_3 = deep reflections; LE and LW = intersection of the cross-section with in-line profiles LE and LW. (For each shot-point–station couple, the reflection point was plotted at mid-distance on a map, then projected onto the closest cross-section; the same projection technique was applied to refracted waves.) 1 = Tertiary molasse; 2 = Urgonian limestone; 3 = Tithonian limestone; 4 = *Terres Noires*; 5 = pre-Triassic basement. (The surface geology for the Chartreuse part of the three lower sections is largely inspired by Gidon 1985.)

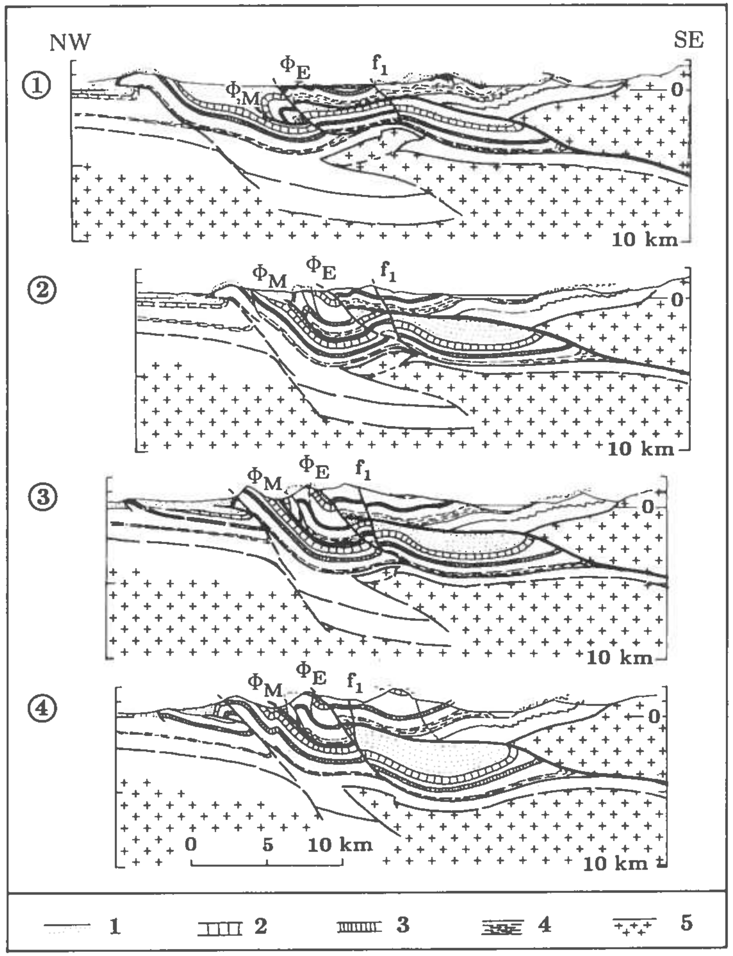

Fig. 9. Deep structure of northern Chartreuse along the four cross-sections of Fig. 8, integrating the deep seismic sounding results. Φ_E, Φ_M and f_1 = overthrusts and strike-slip fault (see map, Fig. 10; and see Fig. 8 caption for a full description of the geological units). Note: (i) the large extent of the median overthrust Φ_M, connected to the overthrust of the Belledonne crystalline unit (upper right part of the sections); (ii) the complex geometry of the sedimentary series under Φ_M; (iii) the maximum depth of 8 km reached by the pre-Triassic basement in the central part of the sections, with a 2 km thick Palaeozoic cover (reflections R_2 and R_3); (iv) the seismic results do not support a strong dip of the Subalpine basement units; towards the NW, the sediment thickness would then decrease stepwise rather than continuously, involving one—or several ?—basement fault(s).

and 13. The refraction level is deeper than before, while the R_1 reflection level—different from the latter—is between 5.0 and 5.6 km. Reflection R_2 can be seen in Fig. 7 gently dipping to the SE at a depth of about 8 km. This is, beyond a doubt, one of the major phases on the record-section and will thus contribute to the identification of reflector R_2 with the pre-Triassic basement. Still deeper, reflector R_3 is sited at a depth of 10 km.

A final remark concerns the easternmost traces of fan F_2 (Fig. 6), where no reliable correlation can be traced for reflected waves. The corresponding stations, on the eastern bank of Isère river, are located on the Liassic and Jurassic cover of Belledonne and on the Belledonne crystalline outcrop itself. The shallow position of the crystalline basement ahead of Belledonne induces a cross-dip effect which is difficult to quantify but which is clearly seen on the section, with a refracted wave making arrival times up to 0.5 s earlier. Thus, a basement at very shallow depth ($\approx$1.5 km) can be expected south of the junction between the Isère valley and the Chambéry cross-valley.

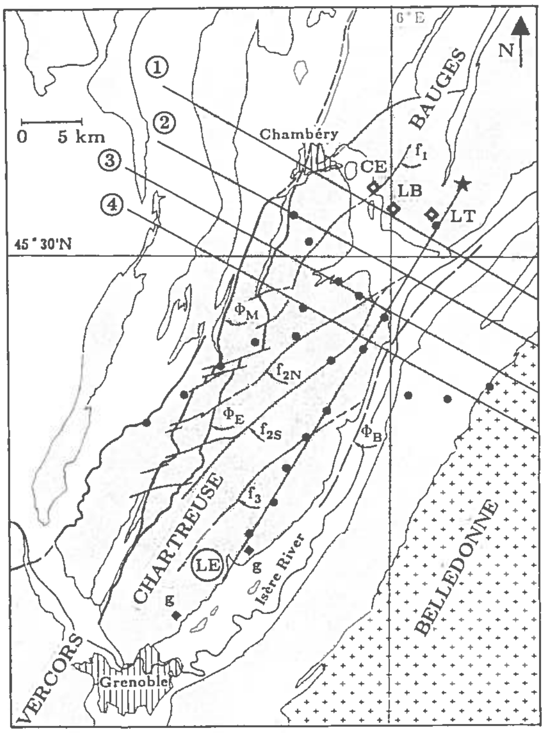

Fig. 10. Surface faulting and overthrusts in Chartreuse. Shaded: Mesozoic terrains. Strike-slip faults (f_1, f_{2N}, f_{2S}, f_3); main thrusts (Φ_E = eastern thrust, Φ_M = median thrust, Φ_B = leading edge at depth of the Belledonne thrust); thermomineral springs (CE = Challes-les-Eaux, LB = La Boisserette, LT = La Thuile) shown as open diamonds; natural gas emergence (southern Chartreuse) shown as a full diamond. LE = in-line profile, re-interpreted in Fig. 11. Full circles mark recording stations of the explosion-seismology experiment.

INTERPRETATION

Against a local geologic background, the detected seismic discontinuities can be identified as follows (Figs. 8 and 9): the refraction level is the parautochthonous Urgonian limestone; reflectors R_1–R_3 are all related to the pre-Triassic basement, i.e. Palaeozoic cover and/or upper crust. Reflector R_1 is the parautochthonous basement which overthrusts reflector R_2—the autochthonous basement—while reflector R_3 is the autochthonous upper crust itself, underlying a 2 km thick Palaeozoic cover.

Of course it could be thought that the refraction level is the pre-Triassic basement itself, the velocity value of 5.3 km s^{-1} found for the refracted wave being lowered as a result of weathering and a possible cross-dip. Two results can, however, be used to argue against this hypothesis: first, mean velocities computed for the deep reflections keep to the classical values of the sedimentary filling in the region; second, the shallow depth of the refractor under the westernmost stations of fan F_1 would then imply that the basement itself underlies the Oxfordian *Terres Noires*. This does not seem very likely for tectonic reasons, so we do not support it, although we do not have any definite disproof.

Our interpretation infers that northern Chartreuse and southern Bauges terrains are part of a very extensive overthrust at depth with a décollement level in the *Terres Noires*. The top of the parautochthonous series underneath is the Urgonian slab, possibly overlain with Tertiary molasse, while the footwall is the pre-Triassic basement.

Where does this overthrust outcrop?

A two-fold possibility (Figs. 9 and 10) is offered through the well-documented eastern Chartreuse thrust (Φ_E) and median Chartreuse thrust (Φ_M). Available surface geology data farther south in the Guiers Mort valley show how the Urgonian syncline terminates under Φ_E. Referring to this Urgonian level, the eastern thrust overlap would only be 2 km. Connecting the proposed thrust to Φ_M would therefore be the only possible way to account for the large displacement expected for the overthrust.

The main structural consequence is a considerable modification of the shortening value in the cover of the Subalpine chains. Siddans (1983) and Gidon (1985) estimated a 10 km shortening from surface geology data. In our interpretation the minimum shortening value would be 23–26 km (Fig. 8) with about 17.5 km being absorbed by the main thrust. This value is consistent with the amount of shortening necessary to explain the crustal thickening beneath the ECMs (Ménard & Thouvenot 1984, 1987, Mugnier *et al.* 1987). Finally, it should be stressed that Doudoux *et al.* (1982) had already introduced such a nappe into their sections of the Bauges and Bornes massifs farther north.

Geometry of the parautochthonous series

To compute approximate depths of the refractor—parautochthonous Urgonian—under the stations, two parameters have to be adjusted: the refractor depth under the shot-point and the true seismic velocity of the refractor. When scanning a substantial set of depth–

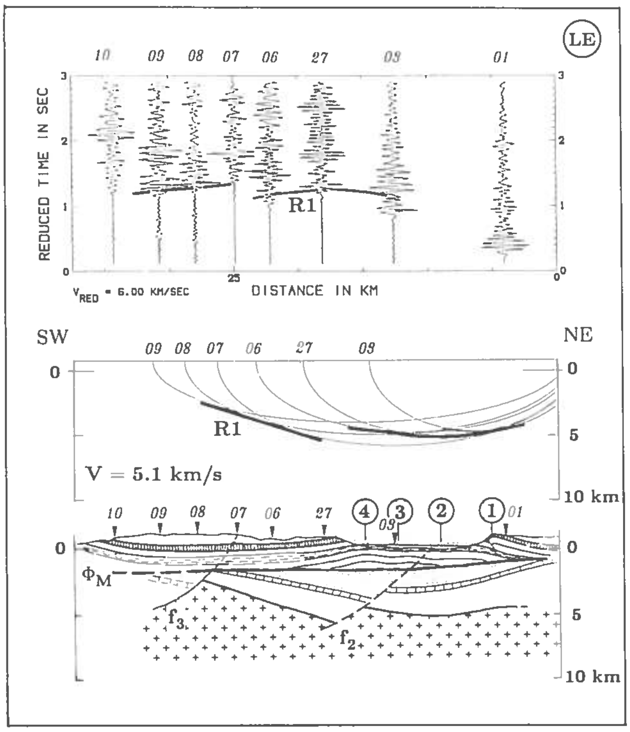

Fig. 11. Re-interpretation of in-line profile LE. Upper part: reduced-time (6 km s^{-1}) record-section, with the new identification of the reflection R_1. Central part: for each shot-point–station couple, the measured reflection time allows us to draw an ellipse with the shot-point and the station as foci, which is the locus of all possible reflection points; this allows to take dip variations into account. The mean velocity above the reflector was fixed at 5.1 km s^{-1}. Lower part: geological interpretation, with two basement units separated by a fault. Φ_M, f_2 and f_3 = overthrust and strike-slip faults (see map, Fig. 10); circled figures refer to the cross-sections in Figs. 8 and 9; see Fig. 8 caption for a full description of the geological units.

velocity couples and stating the further tectonic condition that *the refractor depth cannot be less than* 1 *km*, one is led to choose a model with a refractor 1.8 km deep under the shot-point and a true velocity of 5.4 km s^{-1}. The apparent value of $\approx$5.3 km s^{-1} measured on the in-line profiles would, therefore, be the result of a slight dip of the refractor towards the SW. The minimum depth of 1 km is a limit beyond which there would be no place left for the *Terres Noires* series—see balanced cross-section 2 in Figs. 8 and 9.

With these values, and keeping in mind this deliberate choice based on local tectonics, the following depths can be computed for the refraction level: on fan F_1, it tops under station 20 at 1 km, while it bottoms at 3.4 km under station 03; on fan F_2, it is slightly deeper, between 2.4 (station 25) and 4.1 km (station 27).

On fan F_1 between station 20 and station 12, the wave refracted from the Urgonian level, as well as the basement reflections, are affected by an important offset (Fig. 5). This shows that the series are faulted with a complicated geometry. A straightforward explanation would be a normal-fault scar from Liassic and/or Oligocene extension, with a downwards motion of the south-eastern block. The fault, identified on the surface as f_1 (Fig. 10), has a strike of about N 40°; it could have been re-activated as a strike-slip fault to accommodate the overthrusts. Similar faulting can be recognized all over Chartreuse, e.g. f_{2N}, f_{2S} and f_3 in Fig. 10, the traces of which can be seen on the in-line profile LE—this line intersects the surface faults while LW does not. A revision of our previous line-drawing for reflection R_1 shows that data are indeed consistent with a large basement fault connected to f_2 (Fig. 11).

Oil implications

The Jurassic series of the Dauphinois zone have long been recognized as potential parent rocks for hydrocarbons, especially the Liassic schists and the Oxfordian *Terres Noires*. However, although well-known natural gas emergences can be found in eastern Vercors and Chartreuse, the previous structural models took no account of deep-seated traps.

The existence of a surface overthrust in Chartreuse, which might extend to the Bauges massif, opens up a wide field of possibilities for discovering oil traps in the lower unit, with the footwall of these series being the *Terres Noires* impermeable barrier. The only process likely to have affected the Urgonian level by vertical faulting is Oligocene extension, well-documented in the Bas-Dauphiné—the area between Grenoble and Lyons—where Oligocene semi-grabens overlain with Miocene molasse are common. The same structures are likely to be found here in the lower tectonic unit, under the surface overthrust.

Strong support for this theoretical speculation is brought about by geochemical analyses of thermomineral spring waters in the southern Bauges massif: Challes-les-Eaux, La Boisserette and La Thuile (Fig. 10). Dazy & Grillot (1981) demonstrated the peculiarity of these waters which are enriched with sodium, halides (F^-, Br^-, I^-, Cl^-) and especially sulphur. An isotopic study also shows that sulphates and sulphides are enriched with heavy sulphur isotopes. The high rate found for sulphates is similar to that commonly observed in oil waters or in salt dome cap rocks. Dazy and Grillot (1981) explained this water mineralization in terms of solution processes in the Triassic terrains. It might equally well proceed from the Oligocene series under the surface overthrust.

CONCLUSIONS

The new seismic data presented here do not have the prestige of the stacked sections produced by vertical-reflection seismics—hence the geometrical constraints we derive should not be overemphasized. The way we proceeded here, trying to reconcile the observation of each seismogram with a general idea of the local tectonics, can be considered as a kind of inversion of seismic data in which the *a priori* starting model dominates the structure finally proposed. To dominate does not mean to try to fit the data to the model; and our results—most of them unexpected—answer for the probity of the approach. In complex tectonic settings, this kind of seismic data is just another jig-saw piece which has to fit with mapping, tectonics, geochronology and geochemistry to reveal a total picture.

In the central part of the experiment field, we found, as expected, a deep horizon at 8 km which is identified as the pre-Triassic autochthonous basement. Another reflector at 10 km could be due to a 2 km thick Palaeozoic cover. An unexpected result is the evidence of an intermediate parautochthonous basement unit (≈4.5 km deep) which underlies the Belledonne crystalline unit. This last unit extends itself at a relatively shallow depth (1.5 km) under the Isère valley. The experiment failed to demonstrate any dip of the deep and intermediate basement units towards the SE, as was previously postulated. One solution is that the autochthonous basement was probably affected by faulting, thus accounting for the well-documented decrease of the sedimentary thickness towards the NW.

While the existence of basement reflections can still be debated because of the data quality, the shallow refraction level discovered under northern Chartreuse is perfectly clear. Most of the preceding discussion and the cross-sections in Fig. 9 are based on it being associated with the Urgonian limestone slab. The identification of this slab is decisive in the importance we give to the overthrust Φ_M. This would be a major thrust and imply a total cover shortening of 25 km which is much larger than the 10 km previously thought. With the possibility of finding Tertiary molasse pinched under this overthrust, oil traps could occur there, as perhaps signalled by local thermomineral spring water and gas emergences.

Acknowledgements—The seismic experiment was funded by the programme Géologie Profonde de la France (GPF2). We are indebted to A. Hirn (Institut de Physique du Globe, Paris) for providing the recording equipments and field work facilities. J.-L. Veinante (I.P.G.P.) helped to process the data. Local authorities at the shot-point in La Thuile and Chambéry as well as field-crew and headquarter members are gratefully acknowledged. Comments made by an anonymous reviewer were particularly welcome and helped to clarify the text.

REFERENCES

Alpine Explosion Seismology Group 1976. A lithospheric seismic profile along the axis of the Alps, 1975. I: First results. *Pure & Appl. Geophys.* **114**, 1109–1130.

Arpin, R., Gratier, J.-P. & Thouvenot, F. 1988. Chevauchements en Vercors-Chartreuse déduits de l'équilibrage des données géologiques et géophysiques. *C.r. hebd. Séanc. Acad. Sci., Paris* **307**, 1779–1781.

Biberon, B. 1988. Mécanismes et évolution des chevauchements à vergences opposées. Unpublished thèse, Université de Grenoble.

Dazy, J. & Grillot, J.-C. 1981. Le thermominéralisme péri-alpin: exemple de la région savoyarde (France). *Revue. Géogr. phys. Géol. dyn.* **23**, 319–328.

Doudoux, B., Mercier de Lepinay, B. & Tardy, M. 1982. Une interprétation nouvelle de la structure des massifs subalpins savoyards (Alpes Occidentales): nappes de charriages oligocènes et déformations superposées. *C.r. hebd. Séanc. Acad. Sci., Paris* **295**, 63–68.

ECORS-CROPS Deep Seismic Sounding Group 1989a. A new picture of the Moho under the western Alps. *Nature, Lond.* **337**, 249–251.

ECORS-CROP Deep Seismic Sounding Group 1989b. Mapping the Moho of the western Alps by wide-angle reflection seismics. *Tectonophysics* **162**, 193–202.

Gidon, M. 1985. Aperçu sur la construction et la disposition des ensembles rocheux du massif de la Chartreuse et de ses chaînons satellites occidentaux. In: *Chartreuse Souterraine* (edited by Lismond, B. & Drouin, P.). Sect. Spéléolog. Isère, Grenoble, 11–22.

Karner, G. D. & Watts, A. B. 1983. Gravity anomalies and flexure of the lithosphere at mountain ranges. *J. geophys. Res.* **88**, 10,449–10,477.

Ménard, G. 1979. Relations entre structures profondes et structures superficielles dans le Sud-Est de la France; essai d'utilisation de données géophysiques. Unpublished thèse 3ème cycle, Université de Grenoble.

Ménard, G. 1980. Profondeur du socle anté-triasique dans le sud-est de la France. *C.r. hebd. Séanc. Acad. Sci., Paris* **290**, 299–302.

Ménard, G. & Thouvenot, F. 1984. Ecaillage de la lithosphère européenne sous les Alpes occidentales: arguments gravimétriques et sismiques liés à l'anomalie d'Ivrea. *Bull. Soc. géol. Fr.*, 5 *Ser.* **26**, 875–884.

Ménard, G. & Thouvenot, F. 1987. Coupes équilibrées crustales: méthodologie et application aux Alpes occidentales. *Geodinamica Acta* **1**, 35–45.

Mugnier, J.-L. & Ménard, G. 1986. The development of the Swiss Molasse Basin and the evolution of the external Alps: a kinematic model (in French). *Bull. Centres Rech. Explor.-Prod. Elf-Aquitaine* **10**, 167–180.

Mugnier, J.-L. & Vialon, P. 1986. Deformation and displacement of the Jura cover on its basement, *J. Struct. Geol.* **8**, 373–387.

Mugnier, J.-L., Arpin, R. & Thouvenot, F. 1987. Coupes équilibrées à travers le massif subalpin de la Chartreuse. *Geodinamica Acta* **1**, 123–135.

Rybach, L., Bodmer, P., Pavoni, N. & Müller, S. 1978. Siting criteria for heat extraction from hot dry rock: application to Switzerland. *Pure & Appl. Geophys.* **116**, 1211–1224.

Sheriff, R. E. & Geldart, L. P. 1982. *Exploration Seismology*, Vol. 1. Cambridge University Press, Cambridge.

Siddans, A. W. B. 1983. Finite strain patterns in some Alpine nappes. *J. Struct. Geol.* **5**, 441–448.

Thouvenot, F. 1981. Modélisation bidimensionnelle de la croûte terrestre en vitesse et atténuation des ondes sismiques: implications géodynamiques pour les Alpes occidentales. Unpublished thèse Doct.-Ing., Université de Grenoble.

Thouvenot, F. & Perrier, G. 1981. Seismic evidence of a crustal overthrust in the Western Alps. *Pure & Appl. Geophys.* **119**, 163–184.

Winston, P. H. 1981. *Artificial Intelligence*. Addison-Wesley, Reading, Massachusetts.